MBoC | BRIEF REPORT

Serotonin 5-HT$_7$ receptor slows down the G$_s$ protein: a single molecule perspective

Aleš Petelák[a], Nevin A. Lambert[b], and Alexey Bondar[c,d,*]
[a]Laboratory of Structural Biology and Bioinformatics, Institute of Microbiology of the Czech Academy of Sciences, CZ-37333, Nové Hrady, Czech Republic; [b]Department of Pharmacology and Toxicology, Augusta University, Augusta, GA 30912; [c]Department of Molecular Biology and Genetics, Faculty of Science, University of South Bohemia, CZ - 37005, České Budějovice, Czech Republic; [d]Laboratory of Microscopy and Histology, Institute of Entomology, Biology Centre of the Czech Academy of Sciences, CZ - 37005, České Budějovice, Czech Republic

ABSTRACT **The 5-hydroxytryptamine (serotonin) receptor type 7 (5-HT$_7$R) is a G protein–coupled receptor present primarily in the nervous system and gastrointestinal tract, where it regulates mood, cognition, digestion, and vasoconstriction. 5-HT$_7$R has previously been shown to bind to its cognate stimulatory G$_s$ protein in the inactive state. This phenomenon, termed "inverse coupling," is thought to counteract the atypically high intrinsic activity of 5-HT$_7$R. However, it is not clear how active and inactive 5-HT$_7$ receptors affect the mobility of the G$_s$ protein in the plasma membrane. Here, we used single-molecule imaging of the G$_s$ protein and 5-HT$_7$R to evaluate G$_s$ mobility in the membrane in the presence of 5-HT$_7$R and its mutants. We show that expression of 5-HT$_7$R dramatically reduces the diffusion rate of G$_s$. Expression of the constitutively active mutant 5-HT$_7$R (L173A) is less effective at slowing G$_s$ diffusion presumably due to the reduced ability to form long-lasting inactive complexes. An inactive 5-HT$_7$R (N380K) mutant slows down G$_s$ to the same extent as the wild-type receptor. We conclude that inactive 5-HT$_7$R profoundly affects G$_s$ mobility, which could lead to G$_s$ redistribution in the plasma membrane and alter its availability to other G protein–coupled receptors and effectors.**

Monitoring Editor
JoAnn Trejo
University of California, San Diego

Received: Mar 31, 2023
Revised: Jun 5, 2023
Accepted: Jun 13, 2023

INTRODUCTION

Serotonin (5-hydroxytryptamine, 5-HT) is a neurotransmitter that plays a profound role in the function of the nervous system, gastrointestinal tract, and cardiovascular system (Berger *et al.*, 2009). The multifaceted action of 5-HT regulates mood, sleep, cognition, memory, appetite, digestion, body temperature, and vasoconstriction (Guzel and Mirowska-Guzel, 2022). Malfunctions of 5-HT signaling can lead to depression, anxiety, migraine, irritable bowel syndrome, and obsessive–compulsive disorder (Pourhamzeh *et al.*, 2022).

The 5-HT receptor type 7 (5-HT$_7$R) is a G protein–coupled receptor (GPCR) that belongs to the serotonin receptor family and plays a role in several physiological processes, including the regulation of mood, sleep, and cognitive function (Guseva *et al.*, 2014). 5-HT$_7$R may be involved in the mechanism of action of antidepressant medications (Hedlund, 2009) and has been studied as a potential target for the treatment of a variety of psychiatric conditions, including depression, anxiety, and insomnia (Gasbarri and Pompili, 2014), as well as intestinal disorders (Kim and Khan, 2014).

Unlike most GPCRs, 5-HT$_7$R has been shown to bind to its cognate stimulatory G protein (G$_s$) in the inactive state (Andressen *et al.*, 2018; Ulsund *et al.*, 2019; Jang *et al.*, 2020). This interaction, termed "inverse coupling," is likely required to counteract the outstandingly high basal activity of 5-HT$_7$R (Jang *et al.*, 2020). Therefore, 5-HT$_7$R stimulation with 5-HT has a twofold effect because it induces the binding of G$_s$ molecules to the activated 5-HT$_7$R, as well as activation and dissociation of preassembled 5-HT$_7$R/G$_s$ complexes. However, the effect of inverse coupling on the localization and mobility

This article was published online ahead of print in MBoC in Press (http://www.molbiolcell.org/cgi/doi/10.1091/mbc.E23-03-0117) on June 21, 2023.

The authors declare no potential conflict of interest.

*Address correspondence to: Alexey Bondar (alexey.bondar@entu.cas.cz).

Abbreviations used: 5-HT, 5-hydroxytryptamine (serotonin); 5-HT$_7$R, 5-hydroxytryptamine (serotonin) receptor type 7; CHO-K1, Chinese hamster ovary cells; GPCR, G protein–coupled receptor; G$_s$, stimulatory G protein; Halo, HaloTag; mG$_s$, miniG stimulatory protein; SNAPf, SNAP-tag.

of G_s remains unclear. Here, we used single-molecule imaging of the G_s protein and 5-HT_7R in living cells to determine the effect of 5-HT_7R and its mutants on the mobility of G_s molecules.

RESULTS AND DISCUSSION

We first determined the diffusion coefficients of G_s (when 5-HT_7R was not present) and 5-HT_7R (Figure 1). In experiments with G_s, we utilized the $G\gamma_2$ subunit N-terminally labeled with HaloTag (Halo-$G\gamma_2$) (Los *et al.*, 2008) as described previously (Bondar *et al.*, 2020), expressed at a low level of 0.28 ± 0.19 molecules/μm^2 (mean ± SD) suitable for single-molecule imaging (<1 molecule/μm^2) under control of a minimal promoter (min*P*; Figure 1, A and B). We used the labeled $G\gamma_2$ subunit to avoid alterations that often accompany the labeling of Gα subunits of G proteins (Bondar and Lazar, 2014). To ensure the preferential assembly of the labeled Halo-$G\gamma_2$ in G_s heterotrimers, we also overexpressed nonlabeled $G\alpha_s$ and $G\beta_1$ subunits. G proteins were then fully labeled with the Halo-JF646 dye. Importantly, Chinese hamster ovary cells (CHO-K1) that were used in experiments do not endogenously express 5-HT_7R (Mahe *et al.*, 2004). The 5-HT_7 receptor was labeled with the SNAPf-tag (Keppler *et al.*, 2003) at its N-terminus (SNAPf-5-HT_7R) and overexpressed in CHO-K1 cells. For single-molecule imaging of SNAPf-5-HT_7R, we underlabeled a small fraction of the total 5-HT_7R pool with the SNAP-Surface549 dye (Figure 1, A and C). Single-molecule tracking showed profoundly higher mobility of G_s (observed by imaging Halo-$G\gamma_2$ in presence of overexpressed $G\alpha_s$ and $G\beta_1$) (Figure 1, D and E) in the membrane compared with SNAPf-5-HT_7R (Figure 1E). Initial observed trajectories were segmented into individual tracks using DC-MSS software (Vega *et al.*, 2018) based on the motion type (immobile, confined, free, and directed) exhibited by the segments. The median diffusion coefficient of G_s was 0.292 μm^2/s with 53% of molecules exhibiting free diffusion motion type (Figure 1F). In contrast, SNAPf-5-HT_7R had a median diffusion coefficient of 0.021 μm^2/s with a large fraction of immobile molecules (37%) (Figure 1F). Negligible nonspecific staining was observed with the SNAP-Surface549 dye (200 pM) in control experiments. The median diffusion coefficients obtained from individual tracks (Figure 1G) were consistent with those obtained from individual cells (Figure 1F). The distribution of diffusion coefficients of individual tracks confirmed a higher abundance of low-mobility tracks of SNAPf-5-HT_7R molecules compared with G_s (Figure 1G). These findings show that the G_s protein shows almost 10 times higher mobility than 5-HT_7R ($P < 0.0001$), as expected for membrane-associated and transmembrane proteins, respectively. The striking differences in mobility between these peripheral and integral membrane proteins suggest that the presence of long-lasting complexes between these signaling partners will have a profound effect on G_s mobility.

Next, we set out to determine how 5-HT_7R and its inactive and constitutively active mutants affect G_s mobility (Figure 2). We used the N-terminally SNAPf-tagged wild-type 5-HT_7R, its constitutively active mutant 5-HT_7R (L173A), or the inactive mutant 5-HT_7R(N380K) described previously (Jang *et al.*, 2020). We co-transfected CHO-K1 cells with $G\alpha_s$, $G\beta_1$, and min*P*-Halo-$G\gamma_2$ subunits together with SNAPf-5-HT_7R or its mutants and monitored G_s mobility. As a positive control, we also studied the mobility of HaloTag-labeled mini Gs (mGs), an engineered G protein surrogate that is expected to form long-lasting complexes with active G_s-coupled receptors (Nehme *et al.*, 2017). Typical results of G_s single-molecule tracking are shown in Figure 2, A–C. The median diffusion coefficient of G_s in presence of SNAPf-5-HT_7R was 0.112 μm^2/s, indicating a significant ($P < 0.0001$) decrease in the overall mobility of G_s by 62% and the appearance of a large fraction of immobile molecules (Figure 2, A, F, and I). Diffusion coefficients of these immobile molecules ($D <$ 0.009 μm^2/s) likely indicated limits of detection precision rather than true mobility. The mobility of G_s was less affected in the presence of the active mutant SNAPf-5-HT_7R(L173A) (median $D = 0.181$ μm^2/s) (Figure 2, B, F, and J). G_s mobility in presence of SNAPf-5-HT_7R(L173A) was significantly lower than without a coexpressed receptor ($P = 0.0427$) but higher than in presence of wild-type 5-HT_7R ($P = 0.0229$). However, the expression of the inactive mutant SNAPf-5-HT_7R(N380K) led to a reduction in G_s mobility (median $D = 0.114$ μm^2/s) (Figure 2, C, F, and K) to a similar extent as the expression of the wild-type SNAPf-5-HT_7R (median $D = 0.112$ μm^2/s) ($P > 0.9999$). Both mutants of 5-HT_7R showed mobility similar to that of the wild-type receptor (Figure 2, G and N). As expected, Halo-mGs that appeared in the plasma membrane in cells expressing SNAPf-5-HT_7R (stimulated with 10-μM 5-HT) exhibited very low mobility (median diffusion coefficient 0.039 μm^2/s; Figure 2, D, F, and L) that closely resembled that of the receptor ($P > 0.9999$) and was considerably lower than the diffusion coefficients observed for G_s ($P < 0.0001$). Expression of a prototypical G_s-coupled SNAPf-β_2-adrenergic receptor (SNAPf-β_2AR), which does not exhibit inverse coupling, did not have a significant effect on G_s mobility (Figure 2 E, H, and M) ($P > 0.9999$). The mobility differences obtained from median diffusion coefficients of individual cells (Figure 2F) were confirmed by distinct mobility distributions of individual tracks pooled from all cells in the tested experimental combinations (Figure 2, I–N). G_s tracks exhibited a broad distribution of diffusion coefficients, which consistently shifted toward lower mobility when SNAPf-5-HT_7R variants were present.

Our findings indicate that the presence of wild-type or inactive mutant 5-HT_7R significantly slows the mobility of G_s protein heterotrimers in the plasma membrane, consistent with previous ensemble measurements of G_s mobility (Andressen *et al.*, 2018). This is most likely due to the formation of complexes between the inactive 5-HT_7R and G_s that exhibit the low mobility of the receptor. That G_s mobility remains higher than 5-HT_7R mobility under these conditions suggests that inactive-state complexes are transient (Jang *et al.*, 2020), and there is a fraction of free G_s molecules even in cells overexpressing 5-HT_7R. It is also possible that a small fraction of Halo-$G\gamma_2$ associates with endogenous Gα subunits of other subtypes. Inactive-state complexes do not form when 5-HT_7R is present in its active state, but instead conventional active-state complexes would be expected. Slowing of G_s mobility by the constitutively active 5-HT_7R(L173A) mutant can be explained by such active-state complexes and possibly by receptors that can sample the inactive state despite the activating mutation. It is also possible that binding of activated G_s subunits to slow-moving effectors and regulators could also reduce their mobility (Bondar *et al.*, 2020). In either case, our results are consistent with the suggestion that inactive-state 5-HT_7R-G_s complexes are more stable than active-state complexes (Jang *et al.*, 2020). It remains unclear whether 5-HT_7R forms inactive-state complexes with other G proteins, particularly with the G_{12} protein. Potential roles of membrane domains and endosomal compartments in regulation of abundance and lifetimes of inactive-state 5-HT_7R-G_s complexes remain insufficiently understood. Overall, we conclude that the presence and the activation state of 5-HT_7R have a major effect on the mobility of G_s. This in turn affects the availability of G_s to other binding partners and could affect its spatial distribution in the cellular plasma membrane. For example, clustering of 5-HT_7R in certain compartments of the plasma membrane could cause a selective accumulation of G_s molecules in such areas and their inaccessibility to other partner proteins. Such effects would be

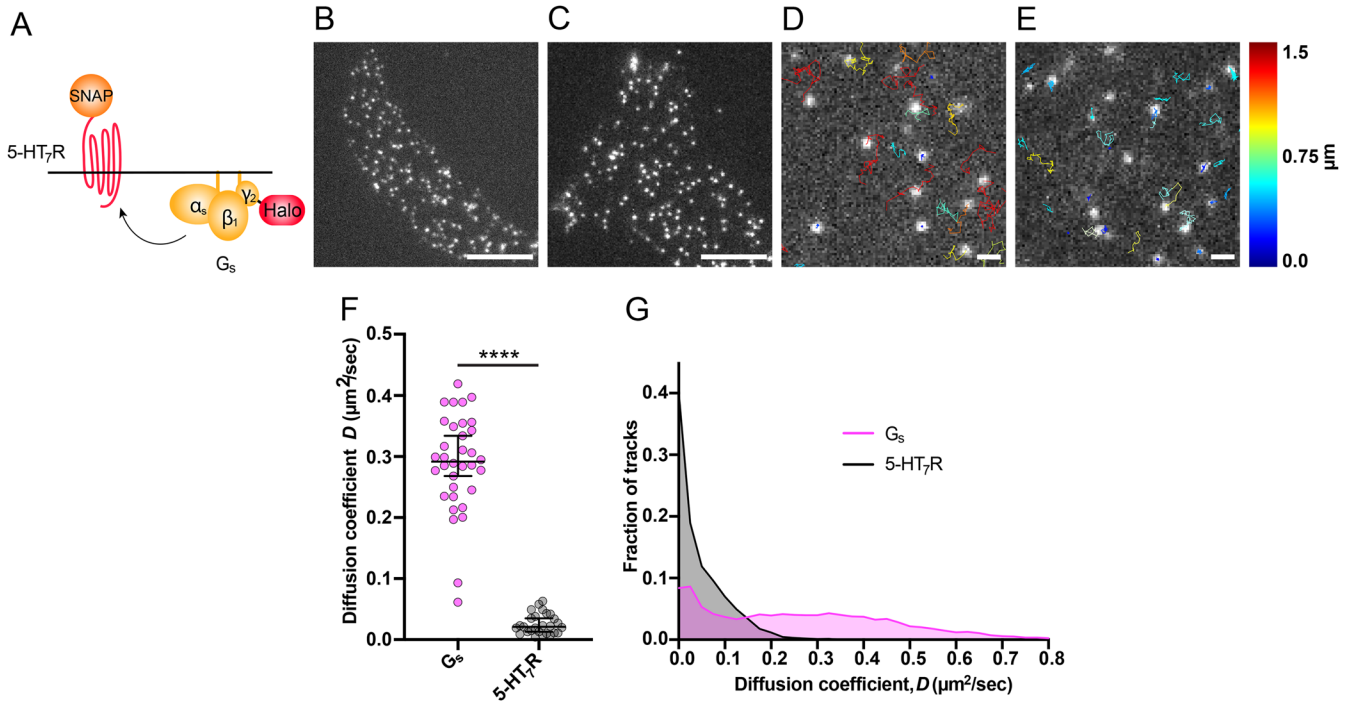

FIGURE 1: Single-molecule imaging of G_s and 5-HT_7R mobility. (A) Experimental design and labeling strategy. The N-terminus of 5-HT_7R was tagged with the SNAP-tag and labeled with the SNAP-Surface549 dye. The G_s protein was tagged at the N-terminus of the $G\gamma_2$ subunit with the HaloTag and labeled with the Halo-JF646 dye. (B) A CHO-K1 cell with low (0.28 ± 0.19 molecules/µm^2 [mean ± SD]) expression of Halo-$G\gamma_2$ fully labeled with the Halo-JF646 dye (50-nM final concentration). (C) A CHO-K1 cell overexpressing SNAPf-5-HT_7R underlabeled with the SNAP-Surface549 dye (200-pM final concentration). Scale bar in B and C 10 µm. (D) Tracks of the Halo-$G\gamma_2$ movement obtained by observation of a cell region for 5 s in the presence of cotransfected $G\alpha_s$ and $G\beta_1$ and in the absence of 5-HT_7R. (E) Tracks of the SNAPf-5-HT_7R movement obtained by observation of a cell region for 5 s in the absence of cotransfected G_s subunits. Scale bar in D and E: 1 µm. The color coding of the tracks in D and E indicates the molecule displacement (as indicated by the color bar). (F) Median diffusion coefficients with 95% confidence interval of individual cells expressing labeled G_s (magenta; $n = 34$, $m = 3$) or 5-HT_7R (gray; $n = 27$, $m = 6$). The receptor demonstrates significantly lower mobility than G_s ($P < 0.0001$, Mann–Whitney test). (G) Comparison of the distribution of diffusion coefficients of individual tracks of labeled G_s (magenta, 10,527 tracks) or 5-HT_7R (gray, 5124 tracks). *n* : number of analyzed individual cells. *m* : number of independent experiments.

expected to depend critically on the overall density of 5-HT_7R in native cells and tissues.

MATERIALS AND METHODS

Request a protocol through *Bio-protocol*.

DNA constructs

Halo-$G\gamma_2$ with expression controlled by the minimal promoter (min*P*, Promega) and SNAPf-β_2AR were described previously (Bondar *et al.*, 2020). Halo-mGs was created by replacing Venus in the Venus-mG_s with HaloTag. The constructs SNAPf-5-HT_7R, SNAPf-5-HT_7R(L173A), and SNAPf-5-HT_7R(N380K) were created by cloning the 5-HT_7R sequence from the PRESTO-Tango GPCR kit (Kroeze *et al.*, 2015) into the SNAPtag-C1 vector and subsequently mutating individual amino acids for the L173A and N380K mutants using Quikchange mutagenesis. Nontagged $G\alpha_s$ and $G\beta_1$ subunits were purchased from cdna.org.

Cell culture

We performed the experiments in CHO-K1 cells (American Type Culture Collection). The cells were cultured at +37°C and 5% CO_2 in the F-12K medium (ThermoFisher Scientific, Waltham, MA) supplemented with fetal bovine serum (Merck, Rahway, NJ) and antibiotic/antimycotic solution (Merck). The cells were passaged twice a week. Cells were plated on plastic six-well plates and cultivated at least 24 h prior to transfection. Transfection was done using PEI-Max (Polysciences, Warrington, PA).

Sample preparation

The preparation of cells for imaging is described in detail in Bondar *et al.* (2020). Briefly, cells were grown and transfected in regular six-well plastic plates. Then 24 h after transfection, cells were washed three times with Dulbecco's phosphate-buffered saline (DPBS) and labeled with Halo-JF646 (50-nM final concentration for full labeling) and SNAP-Surface549 (200 pM final concentration for underlabeling). Cells were incubated with the dyes for 30 min, washed three times with DPBS without Ca^{2+} and Mg^{2+} and dislodged using Accutase (Merck). Dislodged cells were spun three times in DPBS at 300 g for 4 min and plated on extra-clean glass coverslips coated with fibronectin (Merck). Cells were incubated on glass coverslips for 1 h before imaging, which was sufficient for efficient adhesion to the coverslip.

Single-molecule microscopy

Imaging of single molecules was done using Total Internal Reflection Fluorescence (TIRF) microscopy (Axelrod, 1981). We used the Olympus IX83 inverted microscope equipped with the TIRF1

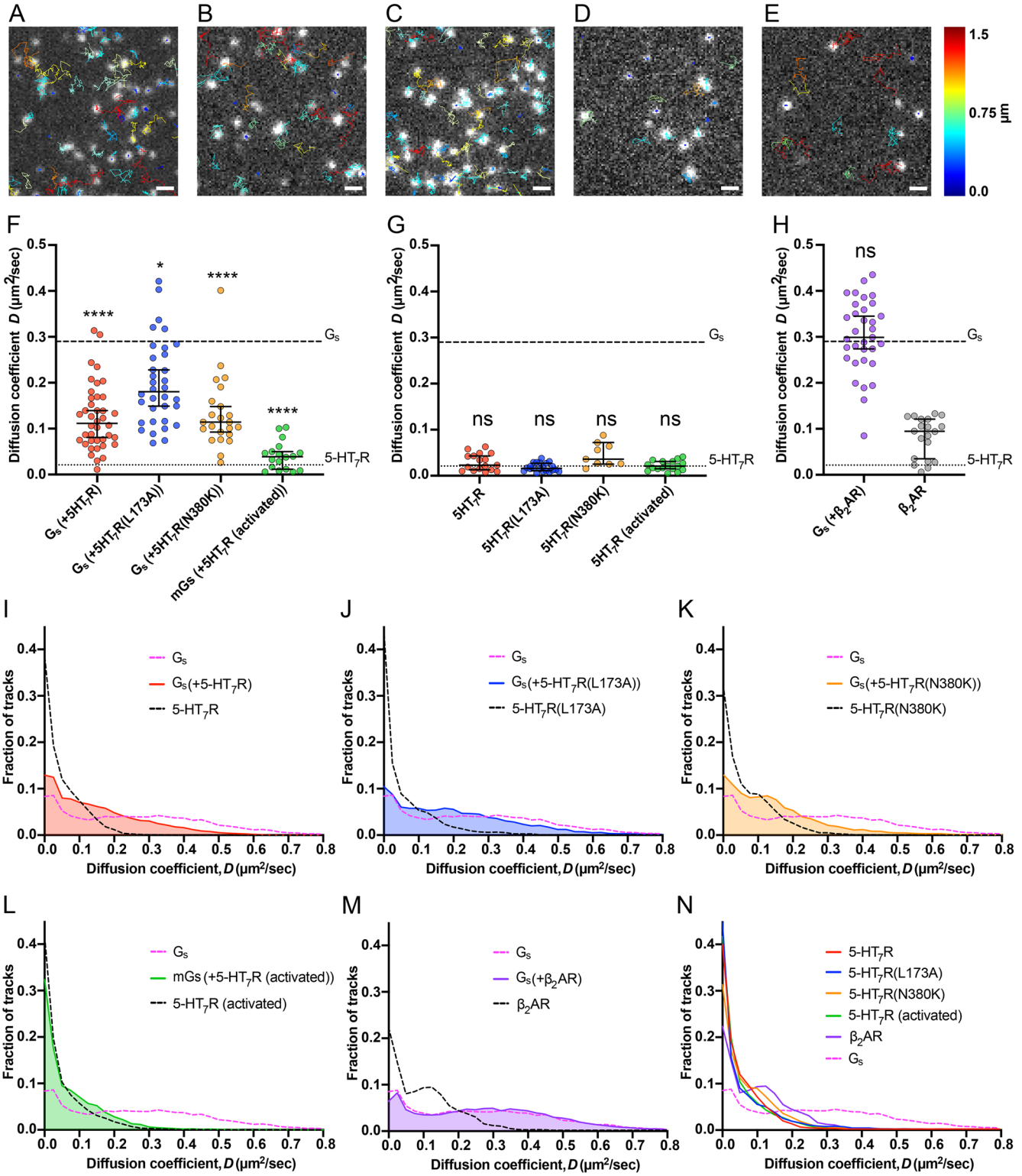

FIGURE 2: Inactive 5-HT$_7$R slows down G$_s$ mobility. (A–C) Tracks of single Halo-Gγ_2 molecules cotransfected with Gα_s and Gβ_1 in presence of SNAPf-5-HT$_7$R (A), constitutively active mutant SNAPf-5-HT$_7$R(L173A) (B), and inactive mutant SNAPf-5-HT$_7$R(N380K) (C). (D) Tracks of Halo-mGs molecules in the presence of SNAPf-5-HT$_7$R stimulated with 10 µM 5-HT. (E) Tracks of single Halo-Gγ_2 molecules cotransfected with Gα_s and Gβ_1 in presence of SNAPf-β_2AR. Scale bar in A–E: 1 µm. The color coding of the tracks in A–E indicates the molecule displacement (as indicated by the color bar). (F) Median diffusion coefficients of G$_s$ with 95% confidence interval in individual cells expressing G$_s$ with SNAPf-5-HT$_7$R (red; $n = 40$, $m = 7$), SNAPf-5-HT$_7$R(L173A) (blue; $n = 34$, $m = 3$), SNAPf-5-HT$_7$R(N380K) (yellow; $n = 23$, $m = 3$), and median diffusion coefficients of Halo-mGs in cells expressing SNAPf-5-HT$_7$R and activated with 10-µM 5-HT (green; $n = 18$, $m = 3$). The median diffusion coefficients of G$_s$ and SNAPf-5-HT$_7$R expressed separately are indicated by dashed lines. G$_s$ is significantly slower when coexpressed with SNAPf-5-HT$_7$R ($P < 0.0001$), SNAPf-5-HT$_7$R(L173A) ($P = 0.0128$),

and SNAPf-5-HT$_7$R(N380K) ($P < 0.0001$) than without a coexpressed GPCR. Similarly, membrane-localized mGs bound to the active SNAPf-5-HT$_7$R is significantly slower ($P < 0.0001$) than G_s without a coexpressed receptor. (G) Median diffusion coefficients with 95% confidence interval of SNAPf-5-HT$_7$R (red; $n = 17$, $m = 5$), SNAPf-5-HT$_7$R(L173A) (blue; $n = 21$, $m = 3$), SNAPf-5-HT$_7$R(N380K) (yellow; $n = 9$, $m = 3$), and activated SNAPf-5-HT$_7$R (green; $n = 17$, $m = 3$) in individual cells. No significant differences in mobility of expressed receptors were found. (H) Median diffusion coefficients with 95% confidence interval of G_s (violet; $n = 33$, $m = 6$) and SNAPf-β_2AR (gray; $n = 20$, $m = 4$) in individual cells expressing G_s in presence of SNAPf-β_2AR. G_s mobility in presence of SNAPf-β_2AR is not significantly different from that in the absence of a GPCR ($P > 0.9999$). (I–M) Comparisons of the diffusion coefficient distribution of individual tracks of G_s with SNAPf-5-HT$_7$R (I; red: G_s [20,044 tracks]; black dashed line: 5-HT$_7$R [3975 tracks]), constitutively active SNAPf-5-HT$_7$R(L173A) (J; blue: G_s [11,966 tracks]; black dashed line: 5-HT$_7$R(L173A) [6480 tracks]), inactive SNAPf-5-HT$_7$R(N380K) (K, yellow: G_s [7566 tracks]; black dashed line: 5-HT$_7$R(N380K) [3448 tracks]), Halo-mGs with activated SNAPf-5-HT$_7$R (L, green: mGs [5893 tracks]; black dashed line: activated 5-HT$_7$R [8542 tracks]), and SNAPf-β_2AR (M, violet: G_s [16,715 tracks]; black dashed line: β_2AR [2499 tracks]). (N) Comparisons of the diffusion coefficient distribution of individual tracks of G_s and all tested GPCRs and mutants. In I–N, the distribution of the diffusion coefficients for G_s expressed separately is indicated by the magenta dashed line. The expression of 5-HT$_7$R strongly reduces the mobility of G_s ($P < 0.0001$). The presence of the constitutively active mutant SNAPf-5-HT$_7$R(L173A) has a smaller effect on the mobility of G_s ($P = 0.0128$). Expression of the inactive mutant SNAPf-5-HT$_7$R(N380K) leads to a reduction of the G_s mobility to a similar extent as the nonmutated 5-HT$_7$R. The mobility of Halo-mGs localized in the membrane in the presence of SNAPf-5-HT$_7$R is considerably lower than that of G_s ($P < 0.0001$) and comparable with the mobility of the receptor itself ($P > 0.9999$). Expression of the SNAPf-β_2AR does not affect G_s mobility ($P > 0.9999$). *n*: number of analyzed individual cells; *m*: number of independent experiments. Statistical testing was done using multiple comparisons nonparametric Kruskal–Wallis test with Dunn's correction.

illuminator, 561-nm and 640-nm lasers (100 mW each), 60 × 1.49NA UApoplan objective lens (Olympus), TRF89901-OL3 TIRF quad-band dichroic beamsplitter (Chroma), Zyla 4.2 sCMOS camera (Andor), and a sample heater (Stable Z, Bioptechs). The 652LP dichroic beamsplitter and the 682/40 emission filter were used for imaging at 640-nm excitation, and the 565LP dichroic beamsplitter and the 605/50 emission filter were used for imaging at 561-nm excitation. Imaging of individual cells was performed for 5 s at 33 fps for the 640-nm channel and 18 fps for the 561-nm channel using the 25-mW laser power. In all experiments involving 5-HT$_7$R constructs, receptor presence was confirmed by imaging.

Data analysis

Detection of single particles and their tracking was performed using the TrackMate plugin (Tinevez *et al.*, 2017) in Fiji using the LoG detector and the simple LAP tracker. The object diameter was estimated to be 0.4 µm. The quality threshold was manually adjusted for individual time series. The maximal linking distance between two frames was set to 0.5 µm. The median filter and subpixel localization were used. Initial trajectories of at least 20 frames were segmented into individual tracks based on their diffusion type. The diffusion coefficients for individual tracks and their diffusion type were determined using the DC-MSS software (Vega *et al.*, 2018) in MATLAB using the default parameters.

Statistical analysis

The median diffusion coefficients with 95% confidence interval were obtained from individual cells and pooled for separate experimental conditions. Individual tracks from multiple cells were also pooled together for verification to produce a median diffusion coefficient based on all tracks. Normality testing was done using D'Agostino & Pearson omnibus k^2 test. Individual datasets where appropriate were compared using two-tailed Mann–Whitney test. Statistical analysis and comparison of multiple experimental conditions were performed using the nonparametric Kruskal–Wallis test with Dunn's comparison of individual conditions.

ACKNOWLEDGMENTS

The authors thank Prof Luke Lavis (HHMI, Janelia Research Campus) for providing the Halo-JF646 dye. This work was supported by National Institutes of Health (NIH) Grants GM130142 and GM145284 (to N.A.L.), the Czech Science Foundation Grant 20-09628Y, and the Czech Ministry of Education, Youth, and Sports Grant Inter-COST LTC20074 (to A.B.).

REFERENCES

Andressen KW, Ulsund AH, Krobert KA, Lohse MJ, Bunemann M, Levy FO (2018). Related GPCRs couple differently to Gs: preassociation between G protein and 5-HT7 serotonin receptor reveals movement of Gα_s upon receptor activation. FASEB J 32, 1059–1069.

Axelrod D (1981). Cell-substrate contacts illuminated by total internal reflection fluorescence. J Cell Biol 89, 141–145.

Berger M, Gray JA, Roth BL (2009). The expanded biology of serotonin. Annu Rev Med 60, 355–366.

Bondar A, Jang W, Sviridova E, Lambert NA (2020). Components of the Gs signaling cascade exhibit distinct changes in mobility and membrane domain localization upon β_2 -adrenergic receptor activation. Traffic 21, 324–332.

Bondar A, Lazar J (2014). Dissociated GαGTP and Gβγ protein subunits are the major activated form of heterotrimeric Gi/o proteins. J Biol Chem 289, 1271–1281.

Gasbarri A, Pompili A (2014). Serotonergic 5-HT7 receptors and cognition. Rev Neurosci 25, 311–323.

Guseva D, Wirth A, Ponimaskin E (2014). Cellular mechanisms of the 5-HT7 receptor-mediated signaling. Front Behav Neurosci 8, 306.

Guzel T, Mirowska-Guzel D (2022). The role of serotonin neurotransmission in gastrointestinal tract and pharmacotherapy. Molecules 27, 1680.

Hedlund PB (2009). The 5-HT7 receptor and disorders of the nervous system: an overview. Psychopharmacology (Berl) 206, 345–354.

Jang W, Adams CE, Liu H, Zhang C, Levy FO, Andressen KW, Lambert NA (2020). An inactive receptor-G protein complex maintains the dynamic range of agonist-induced signaling. Proc Natl Acad Sci USA 117, 30755–30762.

Keppler A, Gendreizig S, Gronemeyer T, Pick H, Vogel H, Johnsson K (2003). A general method for the covalent labeling of fusion proteins with small molecules in vivo. Nat Biotechnol 21, 86–89.

Kim JJ, Khan WI (2014). 5-HT7 receptor signaling: improved therapeutic strategy in gut disorders. Front Behav Neurosci 8, 396.

Kroeze WK, Sassano MF, Huang XP, Lansu K, McCorvy JD, Giguere PM, Sciaky N, Roth BL (2015). PRESTO-Tango as an open-source resource for interrogation of the druggable human GPCRome. Nat Struct Mol Biol 22, 362–369.

Los GV, Encell LP, McDougall MG, Hartzell DD, Karassina N, Zimprich C, Wood MG, Learish R, Ohana RF, Urh M, et al. (2008). HaloTag: a novel protein labeling technology for cell imaging and protein analysis. ACS Chem Biol 3, 373–382.

Mahe C, Bernhard M, Bobirnac I, Keser C, Loetscher E, Feuerbach D, Dev KK, Schoeffter P (2004). Functional expression of the serotonin 5-HT7 receptor in human glioblastoma cell lines. Br J Pharmacol 143, 404–410.

Nehme R, Carpenter B, Singhal A, Strege A, Edwards PC, White CF, Du H, Grisshammer R, Tate CG (2017). Mini-G proteins: novel tools for studying GPCRs in their active conformation. PLoS One 12, e0175642.

Pourhamzeh M, Moravej FG, Arabi M, Shahriari E, Mehrabi S, Ward R, Ahadi R, Joghataei MT (2022). The roles of serotonin in neuropsychiatric disorders. Cell Mol Neurobiol 42, 1671–1692.

Tinevez JY, Perry N, Schindelin J, Hoopes GM, Reynolds GD, Laplantine E, Bednarek SY, Shorte SL, Eliceiri KW (2017). TrackMate: an open and extensible platform for single-particle tracking. Methods 115, 80–90.

Ulsund AH, Dahl M, Frimurer TM, Manfra O, Schwartz TW, Levy FO, Andressen KW (2019). Preassociation between the 5-HT7 serotonin receptor and G protein G_s: molecular determinants and association with low potency activation of adenylyl cyclase. FASEB J 33, 3870–3886.

Vega AR, Freeman SA, Grinstein S, Jaqaman K (2018). Multistep track segmentation and motion classification for transient mobility analysis. Biophys J 114, 1018–1025.